

Paper ID 214  
**COMPUTATION OF TRANSITION TO TURBULENCE ON ROTOR BLADES**  
G. Depommier, D. Alfano, D. Leusink, G. Leymary

Eurocopter  
Aéroport International Marseille Provence  
13725 Marignane Cedex, France  
e-mail: [guillaume.depommier@eurocopter.com](mailto:guillaume.depommier@eurocopter.com)

## ABSTRACT

The position of laminar-turbulent transition of the boundary layer has a significant influence on the performance of a helicopter rotor. Since various transition mechanisms exist, predicting the transition location for CFD simulations is not an easy task. The present study assesses the influence of various computational parameters on the predicted transition location. For these relative comparisons, the Caradonna-Tung rotor will be used. It will be demonstrated that several computational parameters, such as the mesh refinement, turbulence model and numerical scheme, have a significant influence on the predicted transition position. As a final comparison, simulations will be evaluated with respect to the in-flight measurements on a Dauphin rotor in hover.

## 1 INTRODUCTION

Considering a 3D boundary layer over a helicopter rotor blade, the transition position influences in various ways the rotor performance: first of all, the friction drag is directly related to the state of the boundary layer, thereby influencing the rotor torque required. Secondly, flow separations may be allowed or increased in size by boundary layer laminarity. Especially in forward flight, where a dynamic stall region may occur, the transition position may significantly affect the dynamic stall characteristics. To summarize, a correct prediction of the state of the boundary layer, and thus of the transition position, is required for a precise computation of rotor performance.

Despite the significant role of the transition position on performance simulation, its computation with Computational Fluid Dynamics (CFD) simulation is still a challenging topic [1]. Modeling difficulties are from many sources. Classically, various possible causes of transition may be distinguished on a helicopter rotor: Tollmien-Schlichting (T-S) waves, cross-flow instabilities or by-pass transition.

T-S waves are streamwise viscous instabilities initiated from flow disturbances in a process

called receptivity, followed by exponentially increasing instabilities that finally cause breakdown into a turbulent flow. The stability amplification starts when achieving the so-called critical Reynolds number, which is related to the position where the oscillation first becomes unstable [2].

Besides T-S waves, transition may also occur on a helicopter rotor by cross-flow instabilities. On swept-wings, instabilities in the cross-flow direction occur in regions with a strong pressure gradient. This additional instability may cause transition earlier than for a 2D flow [3].

A third transition mechanism probably found on helicopter rotors is by-pass transition. Here, no transient region of instabilities growth can be identified. Instead, transition occurs almost instantaneously and is caused by the high turbulence level of the incoming flow [4]. Since helicopter rotor blades typically rotate close to or in their own wake, this mechanism can be expected to occur over the blades.

In addition to the various transition mechanisms, transition prediction is further complicated by the numerous influences acting on transition: surface geometry and roughness, disturbances in the incoming flow field or even sound [5].

To address these points, several transition models will be tested in the present paper. These models are described in section 2.

To assess the particularities of transition over a helicopter rotor blade, various measurements have been performed in the past. These include measurements of the transition location in hover on four different rotors [6], hot-wire measurements on the 7A rotor in forward flight [7] and in-flight measurements on the Dauphin rotor in hover [8].

The present paper will use these Dauphin measurements for a final verification. Before doing so, the transition models available in the *e/sA* CFD code [9] will be discussed first. Then, the well documented Caradonna-Tung rotor [10] will be used for studying the effect of multiple computational parameters on the transition position prediction. Even though no transition measurements were performed on this rotor, pressure distributions were measured at 5 spanwise positions on both the upper and lower surface. After validation of the computations with these measurements, the effect of each computational parameter will be assessed by relative comparison. These computations can additionally be compared to those performed by Shaw, Hill & Qin [11].

## 2 TRANSITION MODELS

The state of the boundary layer can be expressed by the intermittency function  $\gamma$ . For eddy viscosity turbulence models, as used here, this function can be considered as a weighting function of the turbulent viscosity, being 0 for a laminar boundary layer and 1 in turbulent flow. The effective viscosity  $\mu_{eff}$  used in the Reynolds-Averaged Navier-Stokes (RANS) equations is expressed as a function of the laminar and turbulent viscosity,  $\mu$  and  $\mu_t$ :

$$\mu_{eff} = \mu + \gamma\mu_t$$

As transition now depends upon the intermittency function, the latter needs to be defined in all mesh nodes close to the blade surface. A first way to define intermittency is simply to impose transition by writing the intermittency values into a file, interpreted by *e/sA*. To predict transition by a model, two ways of modelling intermittency exist: local and non-local models.

Local methods use boundary layer information, such as its thickness and the

pressure gradient, to predict its state. These empirical models are often used for Tollmien-Schlichting instabilities, but they may fail to model other transition mechanisms as no history effects are considered. Local models predict turbulent flow when the local Reynolds number exceeds the computed transition Reynolds number.

$$Re_{\theta local} > Re_{\theta transition}(\Lambda_2, Tu)$$

Where  $Tu$  is the external turbulence level and

$$\Lambda_2 = -\frac{\theta^2}{\mu_e U_e} \frac{\partial p}{\partial s}$$

the local pressure gradient parameter of Pohlhausen, with the subscript  $e$  indicating the edge of the boundary layer.

The two local models tested in the present study are the criteria of Abu-Ghannam & Shaw [12] and Dunham [13], each calibrated for different external turbulence levels.

Non-local methods are based on the use of so-called computation lines, along which the boundary layer evolution is integrated to keep a history effect of the boundary layer. The non-local method used in *e/sA* is the Arnal-Habiballah-Delcourt (AHD) criterion [14]. This criterion is also based on the development of Tollmien-Schlichting laminar instabilities. Transition is again predicted when the critical Reynolds number is reached. This Reynolds number is a function of the Pohlhausen pressure gradient, external turbulence level and the local shape factor. The Falkner-Skan similarity equations are used to represent the laminar boundary layer velocity profiles.

In addition to these models, correction terms may be applied to take into account for compressibility or crossflow. The crossflow correction, expected to be of interest for rotor flow, is tested in the present study.

## 3 RESULTS OF THE CARADONNA-TUNG ROTOR

The Caradonna-Tung rotor [10] has 2 untapered, untwisted blades with a NACA0012 airfoil. All pressure distribution measurements were performed in hover, for various rotational speeds and collective pitch angles. This rotor was used in the computations by Shaw, Hill & Qin [11].

To start comparing the measurements with the present computations, the pressure distributions for 5 radial positions of the measurements and our simulations are given in Figure 1. The computations present pressure distributions in good comparison to the experimental results of Caradonna & Tung, except for an overprediction of the negative  $C_p$  at the leading edge on the lower surface near the blade tip ( $r/R = 0.89$ ).

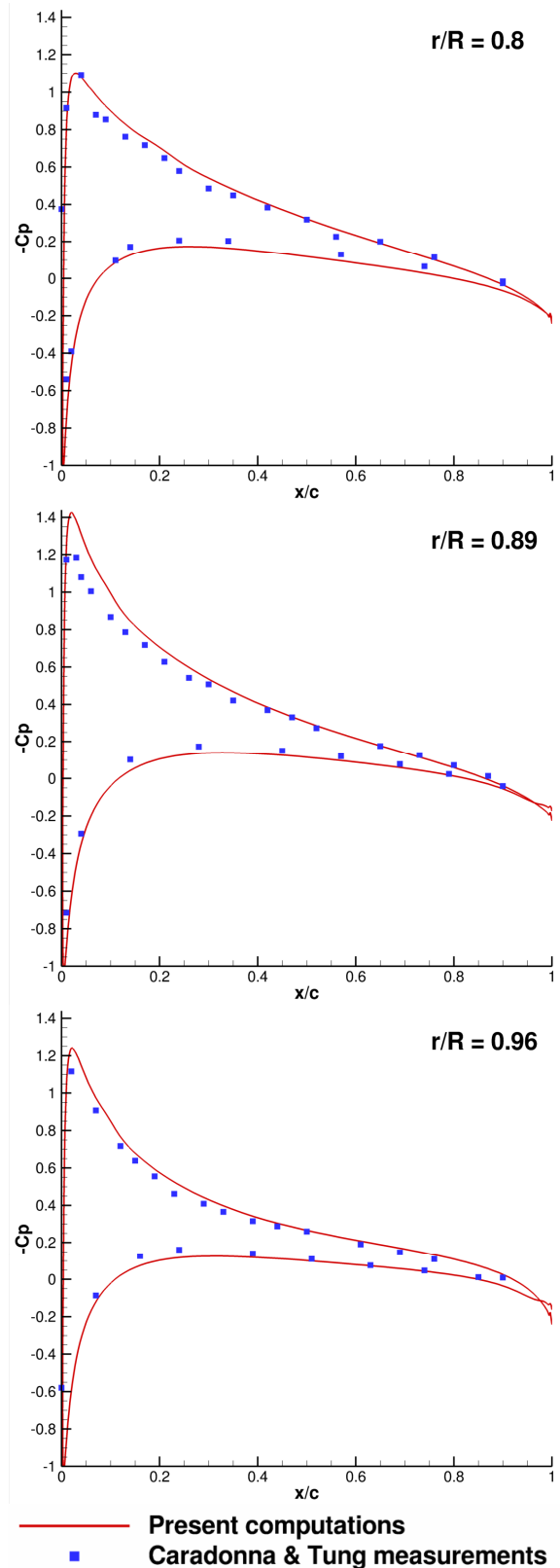
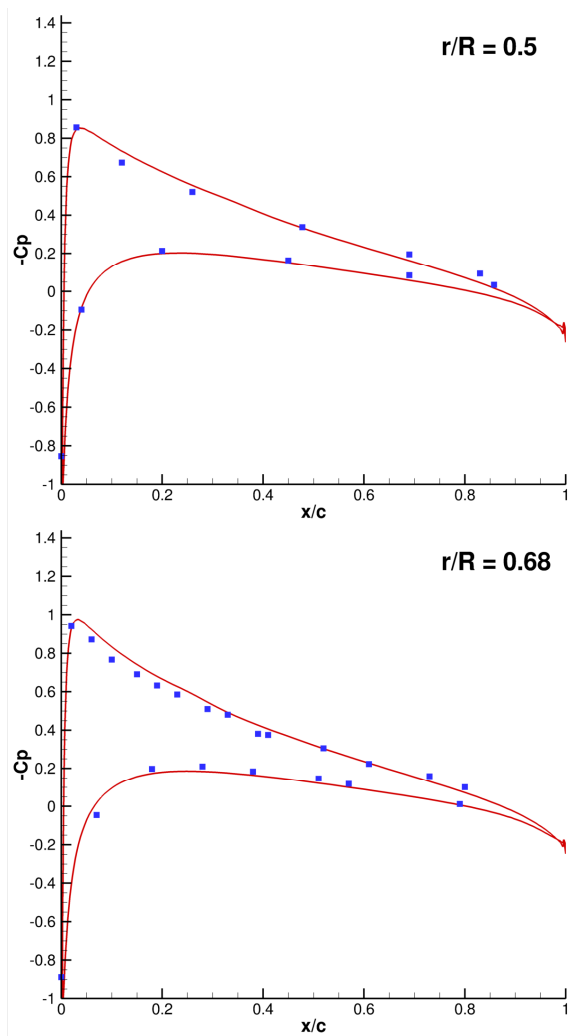


Figure 1: Comparison of pressure distributions of the Caradonna & Tung measurements and present computations for various radial positions

The transition position on the Caradonna-Tung rotor as computed in [11] is compared to the present computations in Figure 2. Transition on a helicopter blade typically occurs close to  $0.8 x/c$  on the lower blade surface, whereas transition on the upper surface is positioned around  $0.2-0.3 x/c$ . For the upper surface of the blade, our computations estimate the transition location to be closer to the leading edge than the 3D-calculations of Shaw, Hill & Qin. This is true as well on the lower surface, except for the blade tip where our calculations predict the transition to be closer of the trailing edge. To conclude, present computations seems to correctly predict the flow around the blades and the transition location prediction is quite similar the Shaw, Hill & Qin results. Therefore this computation is used as a basis for further investigation about different numerical parameters, as presented in the following sections.

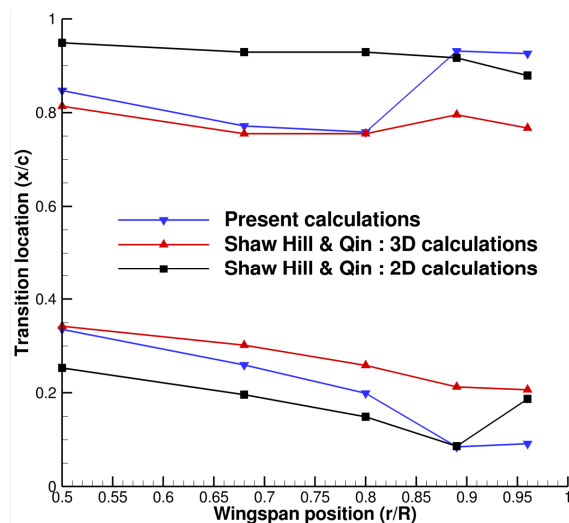


Figure 2: Comparison of the transition location prediction between Shaw, Hill & Qin [11] and Eurocopter computations

### 3.1 Mesh convergence

For the computations a chimera approach was used with a blade mesh and a background mesh as shown in Figure 3. Background mesh contains the blade mesh, which is a C-H mesh built around the NACA0012 blade used for the Caradonna & Tung experiments. Periodic boundary conditions were used for the background mesh in order to reduce its size and to simulate a complete background.

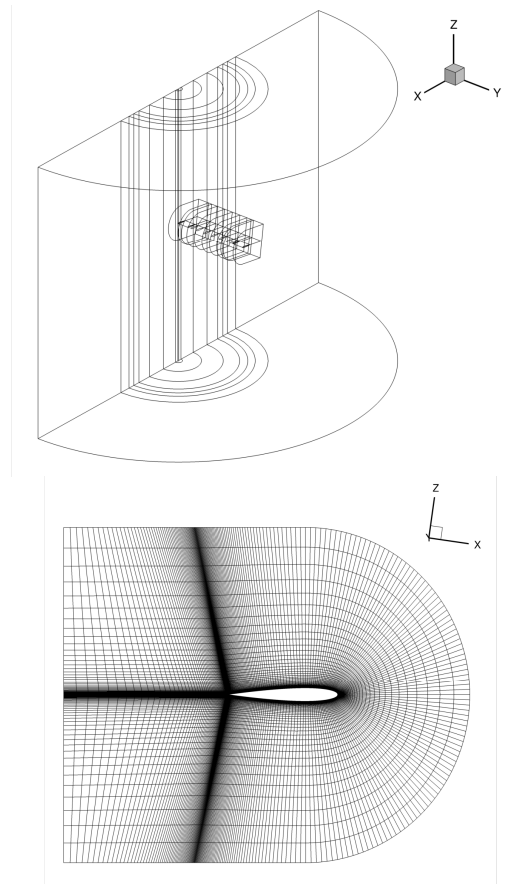


Figure 3: Mesh configuration

In order to correctly predict the transition location, the boundary layer around the blade must be calculated accurately. Given a certain mesh size, the blade mesh density is driven by the following parameters in descending order of importance with regards to gradient calculations:

- the number of mesh points normal to the surface;
- the number of mesh points along the chord (with 53 points behind the trailing edge);
- the number of mesh points along the blade radius.

The length of the first mesh node close to the wall is  $10 \mu\text{m}$  in order to have  $y^+ \approx 1$  close to the blade tip. Given this parameter, simulations were made to estimate the transition calculation sensibility to the mesh density. A Wilcox  $k-\omega$  turbulence model with a Kok correction was used, with a Jameson centred scheme ( $\chi_2 = 0.5$ ,  $\chi_4 = 0.032$ ) for the flux discretization. The transition location prediction was performed by the AHD model with an exterior turbulence level  $Tu$  of 0.01%.

Figure 4 shows the effect of the number of points along the three directions (chord direction denoted  $c$ , normal direction denoted  $n$ , blade span direction denoted  $b$ ). As supposed, adding points along the span direction has less effect than the chord and normal directions except for the blade tip where the 3D effects are stronger. It is also interesting to see that adding more points along the chord moves the transition towards the leading edge, whereas adding more points in the boundary layer moves the transition backwards. For the rest of the present study we will use a c333 n97 b98 blade mesh.

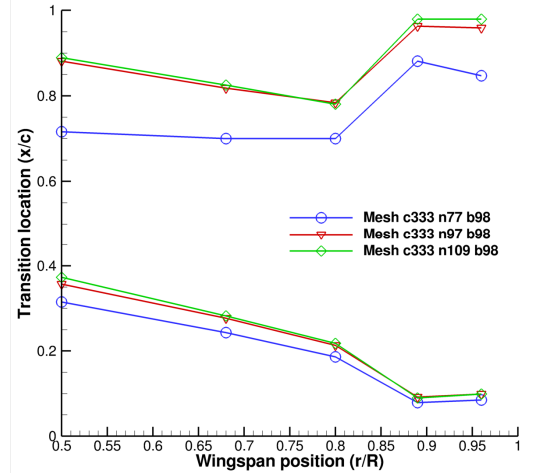
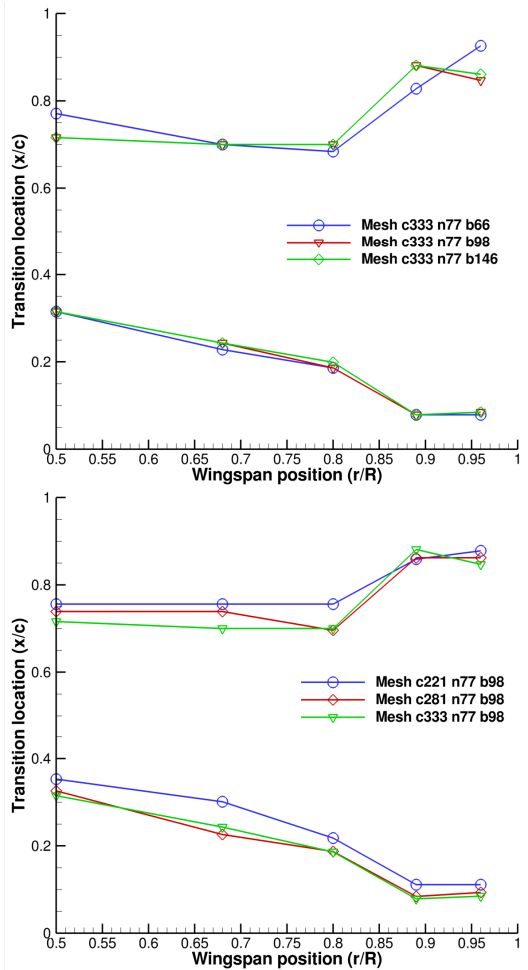


Figure 4: Effect of the mesh refinement on the transition calculation



### 3.2 Effect of turbulence model

As said in the previous section, various turbulence models are available in the *e/sA* code [9] for rotating geometries. The Wilcox  $k-\omega$  turbulence model [15] is a classical model used at Eurocopter. On the other hand, this model is known to be sensitive to the boundary conditions, especially to the dimensionless frequency  $\omega_\infty$  and to the numerical diffusivity damped by the mesh refinement. In order to overcome this sensibility, Kok [16] introduced a cross diffusion term in the Wilcox equations. Another method was proposed by Menter [17] with its BSL hybrid model replacing the  $k-\omega$  classical equations outside the boundary layer by a  $k-\epsilon$  model rewritten in  $k-\omega$  terms. Two classical parameters are used to close the equation system: the turbulent Reynolds  $R_t$  and the flow turbulence level  $Tu$ .

$$Tu = \frac{\sqrt{u'^2}}{U_\infty} = \sqrt{\frac{2k/3}{U_\infty^2}} \quad \text{and} \quad \mathfrak{R}_{t_\infty} = \left( \frac{\mu_t}{\mu} \right)_\infty = C_\mu \frac{\rho_\infty \rho k_\infty^2}{\mu_\infty \epsilon_\infty}$$

The boundary values of  $k$  and  $\omega$  are then obtained by the following expressions

$$(\rho k)_\infty = \frac{3}{2} \rho_\infty U_\infty^2 Tu^2 \quad \text{and} \quad (\rho \omega)_\infty = \frac{\rho_\infty (\rho k)_\infty}{\mathfrak{R}_{t_\infty} \mu_\infty}$$

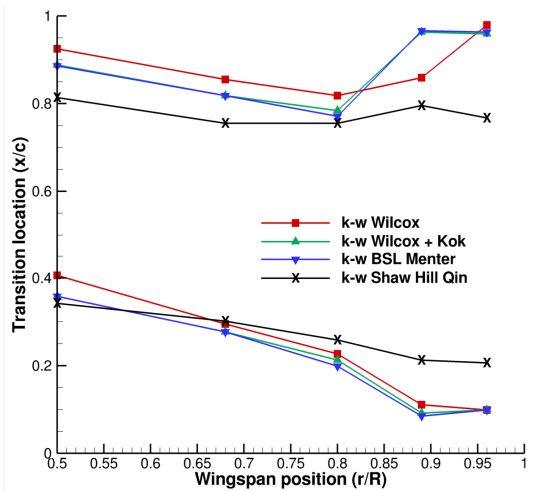


Figure 5: Effect of the turbulence model on the transition location calculation

As we can see in Figure 5, the choice of the turbulence model has a significant effect on the prediction of transition on the lower surface of the blade, especially by the reduction of the sensibility of the k- $\omega$  model to the infinite condition of  $\omega_\infty$  with the Kok correction or the BSL model of Menter. The effect is less pronounced on the upper surface of the blade. On this figure are also plotted the Shaw, Hill & Qin results for the same rotor parameters. The difference between the calculations may have different origins:

- mesh refinement;
- mesh box size;
- boundary conditions;
- transition criterion.

Unfortunately, little information was available on the parameters used, it will be thus difficult to conclude on these differences.

### 3.3 Effect of boundary layer parameters

The external turbulence level  $Tu$  is defined by

$$Tu = \frac{\sqrt{u'^2 + v'^2 + w'^2}}{3 \cdot V}$$

with  $V$  the mean speed of the flow and  $(u', v', w')$  the fluctuating speed components.  $Tu$  is known to modify the instability amplification criterion and thereby has a strong effect on transition. Experimentally,  $Tu$  is directly linked to the wind tunnel quality and changes from one wind tunnel to another. In flight, it is difficult to predict or measure the turbulence level, especially for the flow around a helicopter. That is why calculations were made with different values of  $Tu$  in order to estimate the

transition calculation sensibility to this parameter.

Figure 6 shows that, as expected, a higher turbulence level makes that the transition position moves towards the leading edge for both the upper and lower blade surface. It should be noted that Shaw, Hill and Qin used the Michel transition criterion and were therefore not sensitive to these parameters.

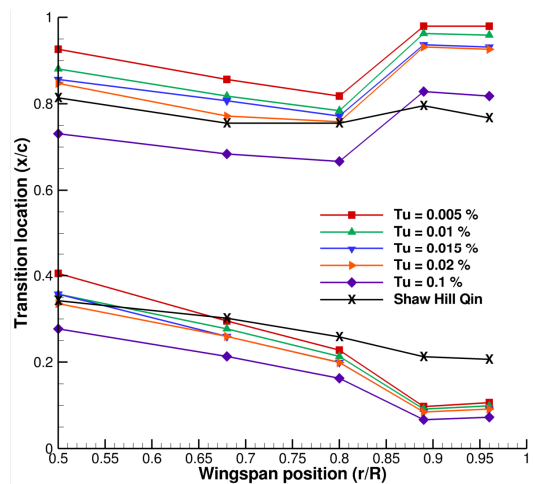


Figure 6: Effect of the external turbulence level  $Tu$  on the transition computation

### 3.4 Effect of transition criterion

The AHD model used for the previous calculations was considered the most advanced criterion available in the flow solver *e/sA* during the study. The results of the transverse effects are presented in Figure 7. A crossflow criterion was added to the AHD model which should have more effect at the blade tip where the pressure difference between upper and lower surfaces creates vorticity.

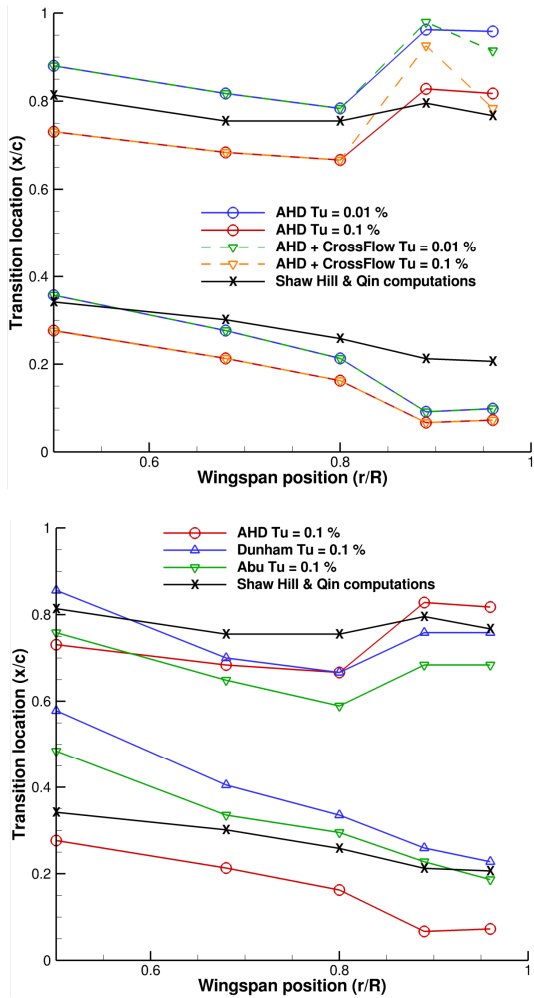


Figure 7: Effect on the transition position of the crossflow terms (top) and of the transition criterion (bottom)

Indeed the crossflow condition has an effect on the transition location, mainly on the lower surface where it delays the transition beyond  $r/R = 0.9$ , advancing it towards the leading edge compared to the AHD criterion alone.

It is also interesting to compare the AHD results to empiric criteria like the Abu criterion or the Dunham one. Those two criteria are linked to the external turbulence level  $Tu$  like the AHD criterion, and allow for making a direct comparison. The results of this comparison are presented on Figure 7. The two criteria tested are predicting a transition closer to the trailing edge than the AHD criterion on the upper surface. On the lower surface this effect is less pronounced as the Abu criterion predicts a transition closer to the leading edge, and the Dunham criterion results are quite similar to the AHD criterion.

### 3.5 Effect of numerical scheme

For each of the previous calculations, a second order centered scheme with Jameson dissipations was used to discretize the convective terms of the flow equations. In very brief, this scheme uses two dissipation coefficients:  $\chi_2$  of order 2 (which should deal with flow discontinuities) and  $\chi_4$  of order 4 (which damps oscillations). These two parameters influence stability and precision of the calculations and their effect on the transition prediction was therefore tested.

Figure 8 presents the results of simulations with different values for  $\chi_2$  and  $\chi_4$ .  $\chi_2$  has less effect on the upper surface than the lower one where it is difficult to conclude. An increase in  $\chi_4$  (thus increasing the dissipation) seems to moves the transition closer to the leading edge.

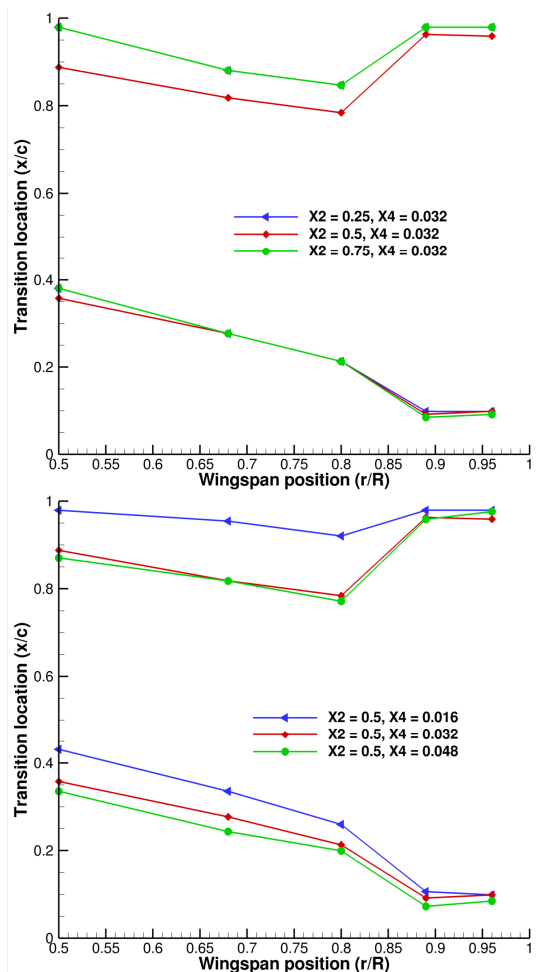


Figure 8: Effect of the artificial viscosity parameters on the transition location

It is also interesting to investigate the effect of another scheme than the centred scheme of Jameson. Other schemes are available in the *e/sA* code, like a AUSM+ upwind code [19] of order 1 raised to the order 2 by a MUSCL method. This scheme does not need any artificial viscosity but requires reference values for temperature, pressure and Mach number. A Van Albada slope limiter is used to keep the TVD property of the scheme. As can be seen in Figure 9, the AUSMP scheme delays transition, shifting it closer to the trailing edge for the upper surface as well as the lower one.

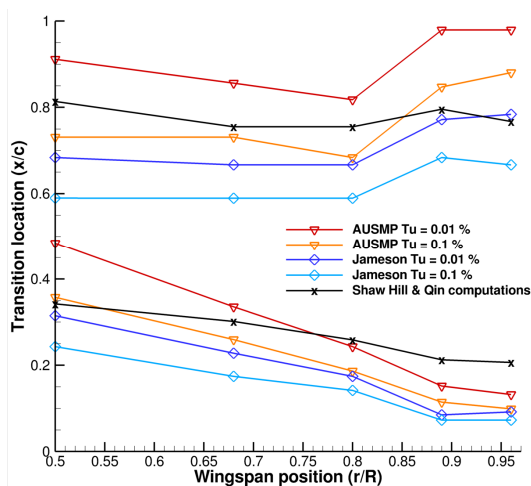


Figure 9: Effect of the flux discretization scheme on the transition location computation

### 3.6 Effect of rotor parameters: rotational speed and pitch angle

Figure 10 presents the results of the transition calculation for various pitch angles. As could be expected, the increase of pitch angle makes the transition move closer to the leading edge on the upper surface because the pressure gradient is more intense and its inversion comes sooner than for lower values of pitch. On the lower surface, the pitch increase has a reverse effect and transition is delayed to the trailing edge.

Figure 10 also presents the results of the simulations for various rotational speeds. Here again the speed increase tends to move transition closer to the leading edge, as the local Reynolds number on the blade increases. The effect of the rotational speed is more significant on the lower surface than on the upper surface.

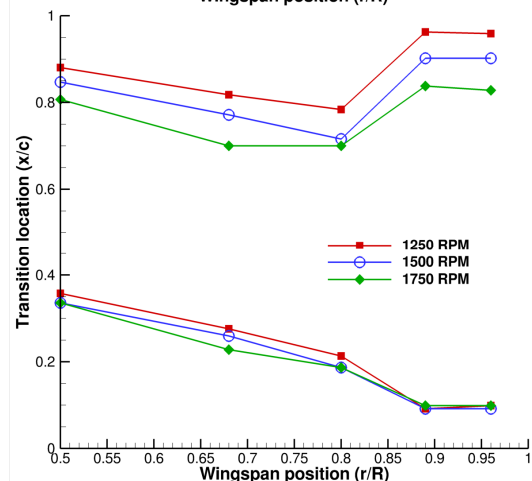
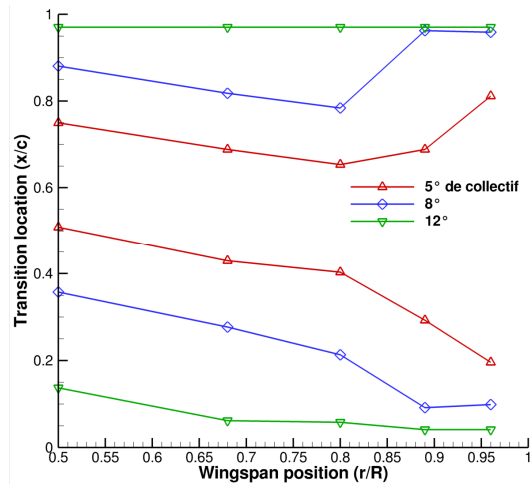


Figure 10: Effect of the rotor parameters on the location of the transition: pitch angle (top) and rotor rotational speed (top)

## 4 DAUPHIN COMPUTATIONS

All previous calculations were made on the NACA0012 rotor of Caradonna & Tung. The same study could be made with a realistic rotor like the Dauphin one for which transition measurements are available.

The Dauphin blade uses OA-profiles and is twisted to keep into account for the spanwise speed evolution. The calculations were made at 350 RPM rotor speed and with a 6.61° collective pitch angle.

We used a c373 n113 b100 mesh for the rotor and used the same background mesh as described before. Like the previous computations a Wilcox *k- $\omega$*  turbulence model with a Kok correction was used, as well as the Jameson scheme. The AHD transition criterion was kept with and without taking into account transients effects with a crossflow condition.

Figure 11 presents the measurements and simulation results. The transition location for the upper surface is rather close the in-flight measurements even though it is difficult to further decide on the best computation parameters. On the lower surface the transition prediction is off with respect to the measurements, especially at the blade tip. In addition, the  $Tu = 0.1\%$  simulations did not succeed in calculating a transition location. This difficulty in predicting the transition location on the lower surface illustrates the persisting complexity of transition predictions, and ask for a better control of testing conditions for such a fine phenomenon (skin roughness for example).

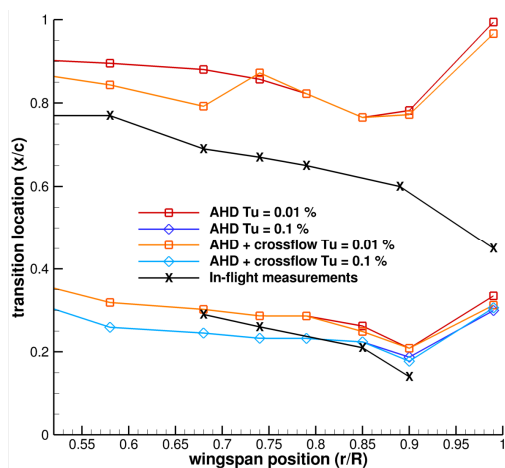


Figure 11: Transition location for a Dauphin rotor

## 5 CONCLUSIONS

The goal of this paper was to investigate the prediction of the transition to turbulence location, and its sensibility to various numerical parameters (e.g. mesh refinement, transition model) and physical ones (e.g. pitch angle, rotational speed). First, the Caradonna & Tung experiments were used as a validation basis of our computations, and the transition prediction were compared to the Shaw, Hill & Qin calculations.

Then different numerical parameters of the computations were tested in order to evaluate their influence on the transition prediction. Mesh refinement has a stronger effect along the chord and within the boundary layer than along the span. The choice of the turbulence model seems to have less effect on the upper

surface than on the lower one. The Menter correction of the Wilcox k- $\omega$  model predicts the transition closer to the leading edge than the other models. It must be noted that the external turbulence level also has a strong impact on the transition calculation, as a higher turbulence level makes that transition occurs earlier. It has also be seen that the choice of the numerical scheme for the convective terms has a strong impact on the transition prediction; using a AUSM scheme makes the transition move closer to the leading edge.

Three different transition models were tested, the AHD model for non-local methods and the Abu and Dunham models for local methods. If the AHD predicts a transition closer to the leading edge on the upper surface, the results for the lower surface are less decisive. The effect of adding a crossflow criterion to the AHD model was also tested.

Finally, physical flow parameters affecting local Reynolds number and pressure gradients were tested, such as the rotor rotational speed and the pitch angle of the blades, an increasing value of both parameters resulting in a transition closer to the leading edge.

After testing each parameter on the Caradonna & Tung rotor, a comparison was made with in-flight measurement of the transition on a Dauphin rotor. While the computations show quite good agreement with the experiments on the upper surface of the blade, the results were off on the lower surface with a computed transition too far from the leading edge.

Without surprise, this study has shown the key role on transition calculation of parameters affecting the boundary layer prediction accuracy. This is especially true for the external turbulence level and the spatial scheme which have often little questioning in industry, and show a large influence on the results.

The second important point to highlight is the lack of refined validation data coming from finely controlled experimental environments. Studies such as the present one have shown the feasibility of transition computations in a pretty complex computing approach (i.e. moving chimera meshes), but little data are available to compare to. Therefore, a

continuous effort on both simulation and experiments concerning transition on rotor blades is still required to really make a breakthrough in the simulation of transition to turbulence on rotor blades.

## 6 REFERENCES

- [1] G. Cheng, R. Nichols, K. D. Neroorkar, P. G. Radhamony: "Validation and Assessments of Turbulence Transition Models", 47<sup>th</sup> AIAA Aerospace Sciences Meeting and Exhibit, Orlando, USA, 5-8 January 2009.
- [2] W. S. Saric: "Introduction to Linear Stability", NATO report n°EN-AVT-151-02.
- [3] H.L. Reed: "Computational Methods for 3-D and Supersonic Flows", NATO report EN-AVT-151-11.
- [4] E. Reshotko: "Transient Growth: A Factor in Bypass Transition", NATO report n° EN-AVT-151-06.
- [5] E. Reshotko: "Paths to Transition in Wall Layers", NATO report n°EN-AVT-151-01
- [6] W. J. McCroskey: "Measurements of boundary layer transition, separation and streamline direction on rotating blades", NASA Technical Note D-6321, 1971.
- [7] Y. Sémézis, P. Beaumier: "Determination of the state of the limit layer on helicopter on helicopter blade sections by use hot films", 31<sup>th</sup> colloque of Applied Aerodynamic, Paris, France, 27-29 March 1995.
- [8] P. Beaumier, C. Castellin, G. Arnaud: "Performance prediction and flowfield analysis of rotors in hover using a coupled Euler/boundary layer method", 24<sup>th</sup> European Rotorcraft Forum, Marseille, France, 15-17 September 1998.
- [9] J-C. Boniface, B. Cantaloube, A. Jolles: "Simulations using an Object Oriented Approach", 26<sup>th</sup> European Rotorcraft Forum, The Hagues, The Netherlands, 26-29 September 2009.
- [10] F.X. Caradonna, C. Tung: "Experimental and Analytical studies of a Model Helicopter Rotor in Hover", NASA Technical Memorandum 81232, 1981.
- [11] S. T. Shaw, J. L. Hill, N. Qin: "Application of Engineering Transition Models to an isolated Helicopter Rotor in Hovering Flight", 43<sup>th</sup> AIAA Aerospace Sciences Meeting and Exhibit, Reno, USA, 10-13 January 2005
- [12] B.J. Abu-Ghannam, R. Shaw: "Natural transition of boundary layers- the effect of turbulence, pressure gradient, and flow history", Journal of Mechanical Engineering Science, 22 (1980), pp 213-228
- [13] J. Dunham: "Prediction of boundary layer transition on turbomachinery blades", AGARD, AG-164, No. 3, 1972.
- [14] D. Arnal, M. Habiballah, E. Coustols: "Laminar instability theory and transition criteria in two- and three-dimensional flows", La Recherche Aérospatiale, 1984-2, pp. 345-365
- [15] D.C. Wilcox: "Turbulence modelling for CFD", DCW Industries, Palm Drive, USA.", 2006.
- [16] J. Kok: "Resolving the Dependence on Freestream Values for the  $k$ - $\omega$  Turbulence Model", AIAA Journal, 38 (7), 2000.
- [17] F.R. Menter: "Two-equation Eddy-Viscosity Turbulence Models for Engineering Applications", AIAA Journal, 32 (8), 1994
- [18] A. Jameson, W. Schmidt, E. & Turkel, "Numerical solution of the Euler equations by finite volume methods using Runge-Kutta time-stepping schemes", 14<sup>th</sup> AIAA Fluid and Plasma Dynamic Conference, 1981
- [19] M.-S. Liou, "A sequel to AUSM: AUSM+", Journal of Computational Physics, Vol. 129: 364-382, article no. 256, 1996